

# Calcium and lanthanide affinity of the EF-loops from the C-terminal domain of calmodulin

Yiming Ye<sup>1</sup>, Hsiau-Wei Lee<sup>1</sup>, Wei Yang, Jenny J. Yang<sup>\*</sup>

*Department of Chemistry, Center of Drug Design, Georgia State University, University Plaza, Atlanta, GA 30303, USA*

Received 1 February 2005; received in revised form 18 March 2005; accepted 25 March 2005

Available online 27 April 2005

## Abstract

To obtain site-specific information about individual EF-hand motifs, the EF-hand  $\text{Ca}^{2+}$ -binding loops from site III and site IV of calmodulin (CaM) were inserted separately into a non- $\text{Ca}^{2+}$ -binding cell adhesion protein, domain 1 of CD2 (denoted as CaM-CD2-III-5G-52 and CaM-CD2-IV-5G-52). Structural analyses using various spectroscopic methods have shown that the host protein CD2 retains its native structure after the insertion of the 12-residue loops. The  $\text{Tb}^{3+}$  fluorescence enhancement upon formation of a  $\text{Tb}^{3+}$ -protein complex and the direct competition by  $\text{La}^{3+}$  and  $\text{Ca}^{2+}$  suggest that native  $\text{Ca}^{2+}$ -binding pockets are formed in both engineered proteins. Moreover, as revealed by NMR, both  $\text{Ca}^{2+}$  and  $\text{La}^{3+}$  specifically interact with the residues at the grafted EF-loop. The CaM-CD2-III-5G-52 has stronger affinities to  $\text{Ca}^{2+}$ ,  $\text{Tb}^{3+}$  and  $\text{La}^{3+}$  than CaM-CD2-IV-5G-52, indicating differential intrinsic metal-binding affinities of the EF-loops.

© 2005 Elsevier Inc. All rights reserved.

**Keywords:** Calcium binding protein; Calmodulin; EF-hand; Metal-binding affinity; CD2

## 1. Introduction

Calmodulin (CaM) is a multifunctional trigger-like protein with a single 148-residue polypeptide chain that controls and regulates many different biological processes [1–5]. Upon increase of intracellular  $\text{Ca}^{2+}$  concentration by hormone and external stimuli, CaM binds to  $\text{Ca}^{2+}$  exhibiting a large conformational change [6]. This  $\text{Ca}^{2+}$ -induced conformational change allows CaM to regulate more than 100 different proteins [7]. Both the crystal and solution structures of CaM show that it is composed of two structurally similar globular domains, the N-terminal and C-terminal domains, linked by a central helix. Each domain contains a pair of  $\text{Ca}^{2+}$ -binding sites (EF-hand) with a 12-residue loop (EF-loop)

flanked by two  $\alpha$ -helices (E and F) [7]. All of the  $\text{Ca}^{2+}$ -binding ligands are located in the EF-loop (Fig. 1), including seven oxygen atoms from the sidechains (positions 1, 3, 5, and 12), main chain (position 7), and a bridged water molecule (position 9). A small anti-parallel  $\beta$ -sheet, formed between the paired EF-loops, plays an important role for highly cooperative  $\text{Ca}^{2+}$ -binding (Fig. 1) [1,2,6]. It is interesting to note that EF-hand proteins use the ubiquitous  $\text{Ca}^{2+}$ -binding motif to coordinate diverse cellular functions in  $\text{Ca}^{2+}$  signaling with different  $\text{Ca}^{2+}$  affinities over a range of  $10^6$ -fold or more [7–11]. Since the activation of CaM is directly related to  $\text{Ca}^{2+}$ -binding, understanding the  $\text{Ca}^{2+}$ -binding properties of CaM has been the focus of numerous studies [12–15]. Different models, such as two classes of  $\text{Ca}^{2+}$ -binding sites [12], four equivalent sites [13–16], and four different sites with similar affinity, have been suggested from early studies of CaM.

$\text{Ln}^{3+}$  ions have ionic radii ( $\text{Tb}^{3+}$  1.06 Å and  $\text{La}^{3+}$  1.05 Å) and coordination properties similar to  $\text{Ca}^{2+}$

<sup>\*</sup> Corresponding author. Tel.: +1 404 651 4620; fax: +1 404 651 2751.

E-mail address: [chejyy@panther.gsu.edu](mailto:chejyy@panther.gsu.edu) (J.J. Yang).

<sup>1</sup> Contribute equally.

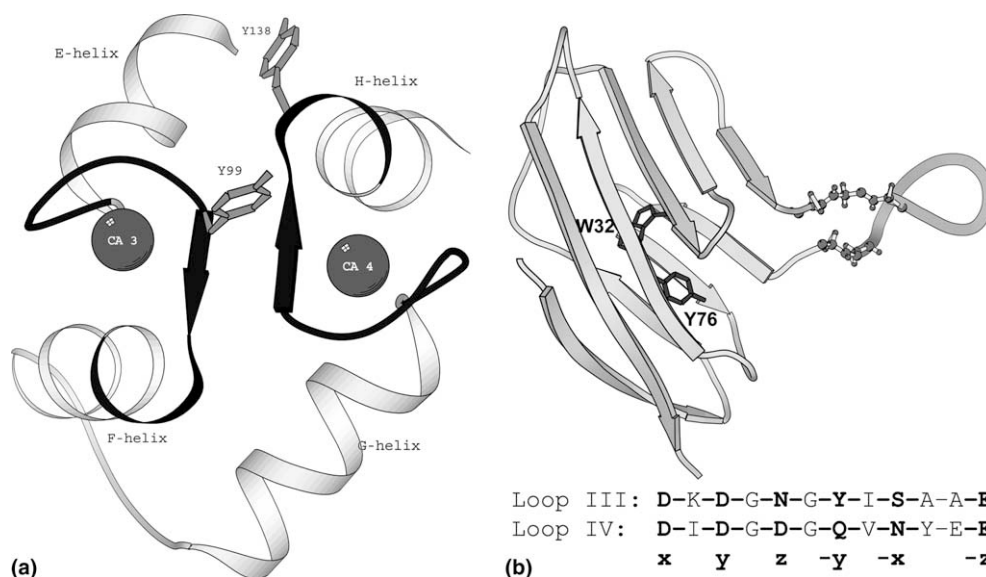


Fig. 1. (a) Three-dimensional structure of the C terminus of CaM (3cln, [48]). The 12-residue loops are in black. The anti-parallel  $\beta$ -strands and two Tyr residues are highlighted. (b) Graphic presentation of domain 1 of CD2 with inserted EF-loop at position 52 of C'D loop.  $\text{Ca}^{2+}$ -binding ligands are highlighted in their sequences and their relative locations are marked below. Two acidic residues are paired at  $z$  axes in CaM loop-IV while no charge pairs in loop-III. The inserted position is  $\sim 15$  Å from Trp-32 and Tyr-76 (Tyr-93 in engineered proteins) in CD2. The figures are prepared using MOLSCRIPT [49].

(0.99 Å). The luminescent members of  $\text{Ln}^{3+}$  have been widely used to sense  $\text{Ca}^{2+}$ -binding proteins through energy transfer (for review see [8,17–19]). When a suitable donor chromophore, such as the aromatic ring of tryptophan or tyrosine, is in proximity,  $\text{Tb}^{3+}$  accepts the energy from the excited donor, and an enhancement of fluorescence at 545 nm is observed. As shown in Fig. 1(a), there is a Tyr residue in each EF-loop with a distance of approximately 15 Å to the  $\text{Ca}^{2+}$  in the X-ray structure of CaM [20].  $\text{Tb}^{3+}$  effectively substitutes for  $\text{Ca}^{2+}$  and has been used to investigate the intrinsic metal-binding properties of individual sites in CaM [21–31]. However, the studies are hampered by the complexities encountered in cooperative binding and the conformational change of coupled EF-hand motifs [12–15] and by a marked decrease in  $\text{Ca}^{2+}$  affinity associated with peptide models due to the penalty of the conformational entropy [32,33].

To obtain site-specific information about EF-hand proteins and to estimate the intrinsic  $\text{Ca}^{2+}$  affinity of the EF-loop in the absence of cooperativity and large conformational entropy penalty, our laboratory has developed a grafting approach in which an isolated  $\text{Ca}^{2+}$ -binding motif with flexible glycine linker is engineered into a stable host protein frame. We have chosen the N-terminal domain of rat cluster of differentiation 2 (CD2) as the “host system” because of its small size, high expression yield, high solubility, and tolerance to mutations. Two Gly linkers (total of five glycines) provide sufficient flexibility of the inserted loop, which is essential for the proper metal binding. In addition, the protein environment has only minor effects on the metal

binding since three different positions for the insertion of loop-III show similar metal-binding affinity [34,35]. Furthermore, the grafted EF-loop functions as an unpaired monomer in solution [36]. In this study, we first obtained the metal-binding affinities of loops III and IV of CaM using the grafting methodology. Then the structural properties and the direct metal interaction of grafted EF-loop in the host protein were investigated.

## 2. Materials and methods

### 2.1. Protein engineering and purification

The EF-loop IV of CaM was engineered and expressed as EF-loop III [34,35].  $^{15}\text{N}$ -labeled proteins were expressed in SV medium (45.6 mM  $\text{K}_2\text{HPO}_4$ , 32.4 mM  $\text{KH}_2\text{PO}_4$ , 0.2 mM  $\text{MgSO}_4$ , and 0.018 mM  $(\text{NH}_4)_2\text{Fe}(\text{SO}_4)_2$ ) with 0.5 g of  $^{15}\text{NH}_4\text{Cl}$  and 5 g of glucose per liter of medium. Single colonies were first inoculated in 2 ml of SV media for 8 h, and then transferred to 100 ml medium for overnight growth before being transferred to 1 l of medium for expression. IPTG (isopropyl- $\beta$ -thiogalactoside, 0.2 mM) was added once an  $\text{OD}_{600}$  of 0.8 was reached. An additional 3 h expression was allowed before harvest. After cell lysis, the fusion proteins in the supernatant were applied on GS-4B beads (Pharmacia) and were cleaved by thrombin on beads after the other proteins were washed out. The eluted proteins were further purified using a superdex 75 column (Pharmacia) followed by a cationic exchange column (Hitrap SP Sepharose) with an increased pH gradient. The

identity of CD2 variants was confirmed by SDS-PAGE and mass spectrometry. The protein concentration was measured with  $\epsilon_{280} = 11700 \text{ M}^{-1} \text{ cm}^{-1}$  for CD2 [37].  $\text{Ca}^{2+}$ -free proteins were prepared by separating the EGTA (ethylene glycol-bis( $\beta$ -aminoethylether)- $N,N,N',N'$ -tetraacetic acid) from a protein-EGTA mixture using an SP column with a pH gradient from 4 to 8. All solutions for metal-binding studies were pre-treated on a Chelex-100 (Bio-Rad) column.

## 2.2. Circular dichroism

The far UV CD spectra were collected using a cell with a 10 mm light-path on a Jasco-710 spectropolarimeter. All spectra were the average of four or eight scans with a scan rate of 50 nm/min. The protein concentrations were 2–6  $\mu\text{M}$ .

## 2.3. Intrinsic Trp fluorescence

Fluorescence experiments were performed using a PTI lifetime fluorimeter and a 1 cm pathlength cuvette. The protein concentration was 2  $\mu\text{M}$ . The emission spectrum was from 300 to 400 nm with the excitation at 283 nm. The slit widths were 2 and 4 nm for excitation and emission, respectively. The  $\text{La}^{3+}$  titration was performed by gradually adding stock solutions (1.0 or 10 mM) with 2  $\mu\text{M}$  protein into a protein sample of 2  $\mu\text{M}$  in 20 mM PIPES-10 mM KCl pH 6.8. About 10–15 min equilibrium was allowed with excitation shutter closed after each addition. The contribution of quenching effect by  $\text{La}^{3+}$  was normalized using the change of wild type CD2 under the same conditions. The addition of 2.5 mM  $\text{La}^{3+}$  into CD2 results in a small change (10%) due to quenching.

## 2.4. Aromatic residue-sensitized $\text{Tb}^{3+}$ energy transfer

Aromatic residue-sensitized  $\text{Tb}^{3+}$  energy transfer was carried out using a 1 cm path-length cell with a protein concentration of 2  $\mu\text{M}$  in 20 mM PIPES-10 mM KCl pH 6.8 at room temperature as described previously [35,38].

## 2.5. Rhod-5N fluorescence competition

The competition study between the proteins and Rhod-5N (Molecular Probe) was performed using a PTI lifetime fluorimeter. The emission spectra (560–600 nm) of 20  $\mu\text{M}$  of Rhod-5N in the absence and presence of 50–100  $\mu\text{M}$  proteins were collected as a function of  $\text{Ca}^{2+}$  concentration in 10 mM Tris-10 mM KCl at pH 7.4 (excited at 552 nm) with 1 cm path length cuvette. The binding constants were obtained by fitting the data using the program Specfit/32 (Spectrum Soft-

ware Associates) with the model assuming that both the dye and the protein bind to  $\text{Ca}^{2+}$  with a 1:1 ratio.

## 2.6. Metal binding monitored by NMR

All NMR spectra were recorded using a Varian Inova 500, 600, or 800 MHz spectrometer with a spectral width of about 13 ppm on  $^1\text{H}$  dimension and 36 ppm on  $^{15}\text{N}$  dimension. The protein concentrations were 0.6–1.0 mM for homonuclear two-dimensional and  $^{15}\text{N}$ -evolved three-dimensional spectra and 0.15–0.3 mM for one-dimensional and HSQC (heteronuclear single-quantum coherence) spectra. Data were processed using Felix98 and analyzed using SPARKY 3 (Goddard & Kneller at University of California). The assignment of apo- and loaded-forms of the protein was achieved using the standard procedures and methods. The previous assignment of CD2 at pH 5 by Driscoll and co-workers [39] was used as a reference in our assignment. An equilibrium time of 30 min was allowed after each addition for the metal titrations using one-dimensional NMR. The metal titrations using  $^{15}\text{N}$ - $^1\text{H}$  HSQC contained 50  $\mu\text{M}$  EGTA at the starting point [40] and the final  $\text{La}^{3+}$  concentrations of 50, 86, 158, 190, 217, 244, 280, 352, 534, 1076, and 5050  $\mu\text{M}$  are obtained during the titration.

## 2.7. $\text{La}^{3+}$ and $\text{Tb}^{3+}$ binding affinity

$\text{La}^{3+}$  and  $\text{Tb}^{3+}$  affinities of proteins were obtained using Trp and  $\text{Tb}^{3+}$  fluorescence, respectively. The  $K_d$  values of proteins were calculated by fitting the metal titration curves, assuming that the changes are from both specific and non-specific binding using the following equation modified from that of single binding process [41]:

$$\Delta S = \Delta S_{\max} \times \frac{([P]_{\text{T}} + [M]_{\text{T}} + k_d) - \sqrt{([P]_{\text{T}} + [M]_{\text{T}} + k_d)^2 - 4[P]_{\text{T}}[M]_{\text{T}}}}{2[P]_{\text{T}}} + C \times [M]_{\text{T}} \quad (1)$$

where  $\Delta S$  and  $\Delta S_{\max}$  are the signal change and the total signal change from the specific binding, respectively;  $C$  is the contribution from the non-specific binding; and  $[M]_{\text{T}}$  and  $[P]_{\text{T}}$  are the total concentrations of metal ions and protein, respectively. The effects from the non-specific binding are simplified to be linear at the experimental metal concentrations since this binding is very weak.

## 3. Results and discussion

### 3.1. Structure of CD2 retained after insertion of EF-loops

The conformations of engineered proteins were monitored using far-UV CD, fluorescence and NMR. As

shown in Fig. 2, the CD and fluorescence spectra of CaM-CD2-III-5G-52 and CaM-CD2-IV-5G-52 are very similar to that of CD2, suggesting that the insertion of EF-loops III and IV of CaM with Gly-linkers does not change the secondary structure and aromatic residue environment of the host protein. This is supported by the close similarity of the one-dimensional  $^1\text{H}$  NMR spectra of the CD2 variants to that of CD2 (data not shown).

The structural perturbation of the host protein by inserted EF-loops was further analyzed using  $^{15}\text{N}$ -labeled proteins and multi-dimensional NMR. The HSQC spectra of both engineered proteins (Fig. 3(a) shows CaM-CD2-III-5G-52) retained most of the dispersed peaks in that of CD2 (data not shown). The assignments of the majority chemical shifts in the absence and presence of metal ions were achieved. The chemical shifts of the residues from the host protein part of CaM-CD2-III-5G-52 are very similar to those of CD2, suggesting that its integrity and packing are maintained after the insertion of the  $\text{Ca}^{2+}$ -binding loops [34].

As shown in Fig. 2(a), the addition of  $\text{Ca}^{2+}$  and  $\text{La}^{3+}$  ions does not result in shape change of the CD spectra of either protein, but only small intensity changes were observed as in natural  $\text{Ca}^{2+}$ -binding proteins such as CaM and troponin C [6]. In contrast to the minor metal-induced intensity change of Trp fluorescence in CD2,  $\text{Ca}^{2+}$  (1 mM) and  $\text{La}^{3+}$  (0.1 mM) reduce the signal about 10% and 40%, respectively (Fig. 2(b)). The greater effects of  $\text{La}^{3+}$  than  $\text{Ca}^{2+}$  have also been observed on extracellular  $\text{Ca}^{2+}$ -binding proteins such as  $\gamma$ -crystallin [42]. However, neither  $\text{Ca}^{2+}$  nor  $\text{La}^{3+}$  shifts the emission maximum of the fluorescence of either CD2 variant, suggesting that their native aromatic environments are not altered. In addition, the excess  $\text{La}^{3+}$  or  $\text{Ca}^{2+}$  results in insignificant change for the majority of the resonances from the host protein part in HSQC spectra (Fig. 3).

Collectively, the overall conformation of the host protein is not perturbed by the addition of metal ions. This differs from natural  $\text{Ca}^{2+}$ -binding proteins such as  $\alpha$ -lactalbumin, CaM, troponin C and parvalbumin, which undergo great conformational changes upon metal-binding. Although the possibility that the host protein CD2 modulates the affinities of the inserted loops cannot be excluded, our engineered proteins minimize the interference from the conformational changes, which allows us to monitor and compare the intrinsic metal-binding affinity of the inserted loops.

### 3.2. EF-loop III has greater affinities than EF-loop IV

$\text{Ca}^{2+}$ -binding dissociation constants of the engineered proteins were obtained by monitoring the fluorescence change of the  $\text{Ca}^{2+}$  dye Rhod-5N in the presence of 50  $\mu\text{M}$  protein [27]. The fluorescence emission at 580 nm of Rhod-5N ( $K_d \sim 100 \mu\text{M}$  under experimental conditions) is enhanced upon  $\text{Ca}^{2+}$  binding with an excitation at 552 nm. The competition binding of  $\text{Ca}^{2+}$  by the proteins results in the delay of the Rhod-5N fluorescence increase. The  $\text{Ca}^{2+}$  affinity for CaM-CD2-III-5G-52 ( $185 \pm 30 \mu\text{M}$ ) determined by the competition assay (Fig. 4(a)) agrees well with that obtained by NMR ( $144\text{--}228 \pm 40 \mu\text{M}$ ) [34]. The affinity for CaM-CD2-IV-5G-52 ( $810 \pm 40 \mu\text{M}$ ) is 4-fold weaker (Table 1). The Trp fluorescence change was used to determine the dissociation constants of  $\text{La}^{3+}$ . Fig. 4(b) shows Trp fluorescence of CaM-CD2-III-5G-52 and CaM-CD2-IV-5G-52 as a function of  $\text{La}^{3+}$  concentrations; these give the  $K_d$ s of  $40 \pm 7$  and  $120 \pm 30 \mu\text{M}$  for the two proteins, respectively.

The  $\text{Tb}^{3+}$ -binding affinities of engineered proteins were obtained by monitoring the  $\text{Tb}^{3+}$  fluorescence at 545 nm. As shown in Fig. 1, EF-loops III and IV have a Tyr residue at the loop positions 7 and 10, respectively.

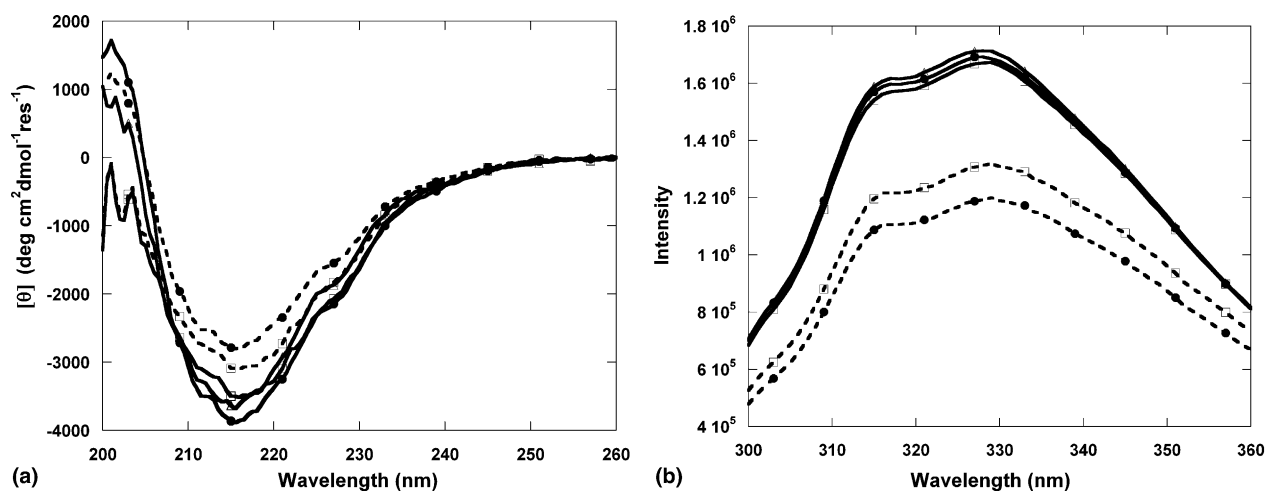


Fig. 2. Far UV CD (a) and Trp fluorescence spectra (b) of CD2 (empty triangle), CaM-CD2-III-5G-52 (filled circle) and CaM-CD2-IV-5G-52 (empty square) in the presence of 1 mM EGTA (solid line) or 0.1 mM  $\text{La}^{3+}$  (dash line) in 10 mM Tris–10 mM KCl, pH 7.4.

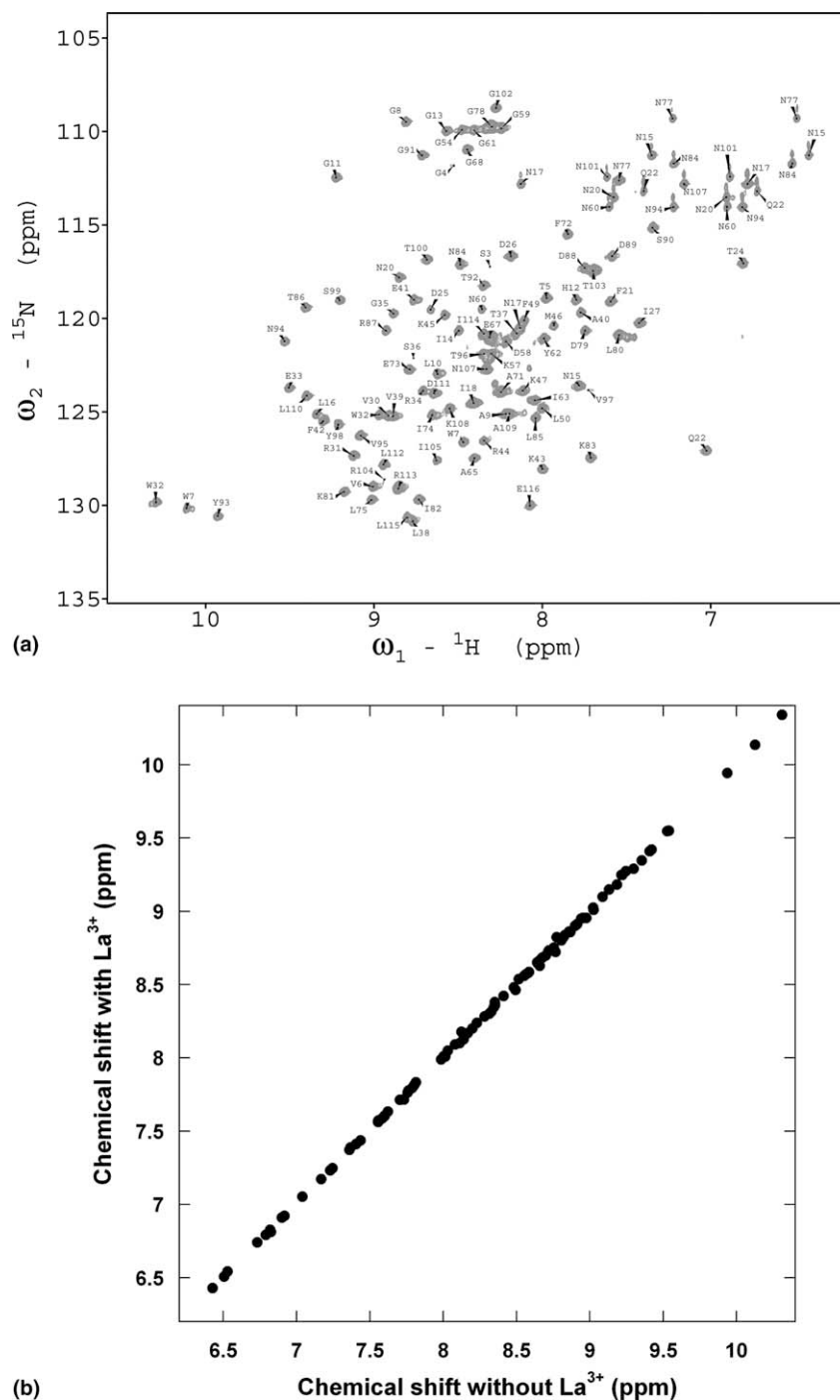


Fig. 3. (a)  $^{15}\text{N}$ - $^1\text{H}$  HSQC spectra of CaM-CD2-III-5G-52 in the absence of metal ions. (b) Chemical shifts of the host protein parts of CaM-CD2-III-5G-52 in the presence of 1 mM EGTA and 1 mM  $\text{La}^{3+}$  in 20 mM PIPES-20 mM KCl, pH 6.8 at 25 °C.

In the model structure of CaM-CD2-III-5G-52 [34], Trp-32 and Tyr-76 in CD2 are about 15 Å away from the insertion location. Engineered proteins are capable of increasing the  $\text{Tb}^{3+}$  fluorescence at 545 nm when excited the aromatic residues. However, this is not observed in CD2; although, it also contains two Trp and two Tyr [34,35]. The  $\text{Tb}^{3+}$  dissociation constant of CaM-CD2-III-5G-52 ( $20 \pm 6 \mu\text{M}$ ) is similar to the peptide fragment of the EF-loop III [32]. The  $\text{Tb}^{3+}$  dissoci-

ation constant of CaM-CD2-IV-5G-52 ( $72 \pm 10 \mu\text{M}$ ) is about 3 fold weaker. Kilhoffer et al. [22] have noticed that the  $\text{Tb}^{3+}$  signal was not significantly increased until the addition of three equivalents of  $\text{Tb}^{3+}$  to the octopus CaM that contains a single Tyr at loop IV, by which they concluded that loop III of CaM has a higher  $\text{Tb}^{3+}$  affinity than loop IV. However, Wallace et al. [21] pointed out that it is difficult to examine the order of  $\text{Tb}^{3+}$  binding because the two EF-loops are close

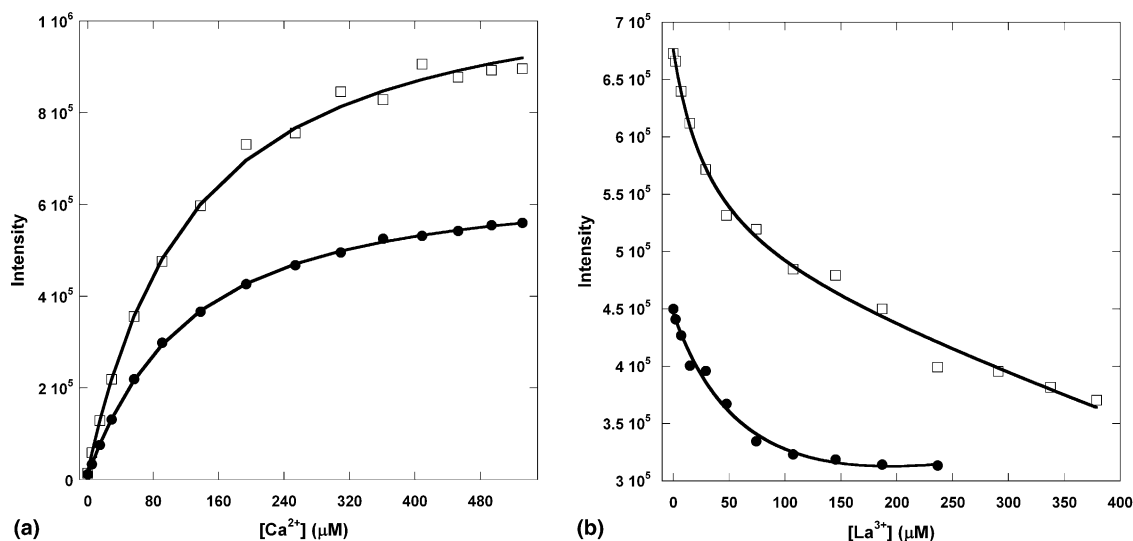


Fig. 4. (a) Rhod-5N emission at 580 nm as a function of  $\text{Ca}^{2+}$  in the presence of 50  $\mu\text{M}$  of CaM-CD2-III-5G-52 (solid circle) or CaM-CD2-IV-5G-52 (empty square) and the global fitting curves (solid line) generated by Specfit 32, assuming both the dye and the protein bind to  $\text{Ca}^{2+}$  with a 1:1 ratio. (b) Change of Trp fluorescence intensity at 327 nm of 2.0  $\mu\text{M}$  CaM-CD2-III-5G-52 (circle) and CaM-CD2-IV-5G-52 (square) as a function of  $\text{La}^{3+}$  concentration in 20 mM PIPES-10 mM KCl, pH 6.8 excited at 283 nm. Solid line is generated by Eq. (1) assuming the formation of a 1:1 metal-protein complex followed by non-specific binding.

Table 1  
Summary of metal-binding affinities

Protein	$\text{Tb}^{3+}$ ( $\mu\text{M}$ ) <sup>a</sup>	$\text{La}^{3+}$ ( $\mu\text{M}$ ) <sup>a</sup>	$\text{Ca}^{2+}$ ( $\mu\text{M}$ ) <sup>b</sup>
CaM-loop III	$20 \pm 6$	$40 \pm 7$	$185 \pm 30$
CaM-loop IV	$72 \pm 10$	$120 \pm 30$	$810 \pm 40$

<sup>a</sup> In 20 mM PIPES-10 mM KCl at pH 6.8.

<sup>b</sup> In 10 mM TrisCl-10 mM KCl at pH 7.4.

enough to allow inter-EF-loop energy transfer in the intact protein. Our grafting approach allowed us to draw the conclusion without such interference.

Taken together, we have shown that CaM-CD2-III-5G-52 has greater affinities than CaM-CD2-IV-5G-52 for  $\text{Ca}^{2+}$ ,  $\text{La}^{3+}$  and  $\text{Tb}^{3+}$ . This contradicts the acid pair hypothesis proposed by Reid and Hodges [43]. They postulated that four acidic residues provide the stable arrangement of anionic charges with the highest  $\text{Ca}^{2+}$  affinity and an EF-hand  $\text{Ca}^{2+}$ -binding site has a stronger  $\text{Ca}^{2+}$  affinity if the anionic ligands are paired on the axial vertices of a near octahedron (i.e., the  $x$  and  $z$  axes) [43]. As shown in Fig. 1, site IV of CaM has one paired charge on the  $z$ -axis with four negatively charged ligand residues while site III has no paired residues with three negatively charged residues. According to the acid-pair hypothesis, the relative  $\text{Ca}^{2+}$ -binding affinity should be  $\text{IV} > \text{III}$ . Reid and co-workers [43–47] have shown that an increase of acidic ligand residues from three to four for the peptide fragment encompassing EF-loop III of CaM enhances the  $\text{Ca}^{2+}$ -binding affinity. However, direct comparison of isolated loops III and IV using peptide fragments was not reported.

Furthermore, the contributions of the loop and that from the other components and cooperativity are difficult to dissect in the intact protein. Our grafted EF-loop in CD2 is well solvated and functions independently of the host protein environment [35]. Therefore, the stronger metal-binding affinity of loop III than loop IV we observed here is likely a reflection of the intrinsic metal-binding properties of each grafted EF-loop.

### 3.3. Metal binding at the inserted loops

To support the idea that the metal affinities we observed reflect the properties of the inserted loop rather than the host protein, NMR has been applied to investigate the engineered proteins. We have assigned 11 residues in the  $\text{Ca}^{2+}$ -binding loop and linker range of CaM-CD2-III-5G-52 (Fig. 3). The cross peak of Glu at loop position 12 (E67) was initially overlapped with that of I114 from the host protein CD2 in the presence of 50  $\mu\text{M}$  EGTA (Fig. 5). Upon the addition of  $\text{La}^{3+}$ , this resonance separated from that of unchanged I114 and moved upfield until overlapping with T37. Furthermore, similar to the intact CaM [31], the addition of  $\text{La}^{3+}$  specifically results in the broadening and change of the chemical shifts from the EF-loop, indicating an intermediate chemical exchange. For example, D58 (at loop position three) disappears upon the addition of  $\text{La}^{3+}$  (Fig. 5). Similar results have been observed for CaM-CD2-IV-5G-52. On the other hand, the addition of either  $\text{Ca}^{2+}$  or  $\text{La}^{3+}$  up to 10 mM does not result in any significant change in the NMR spectra of either wild

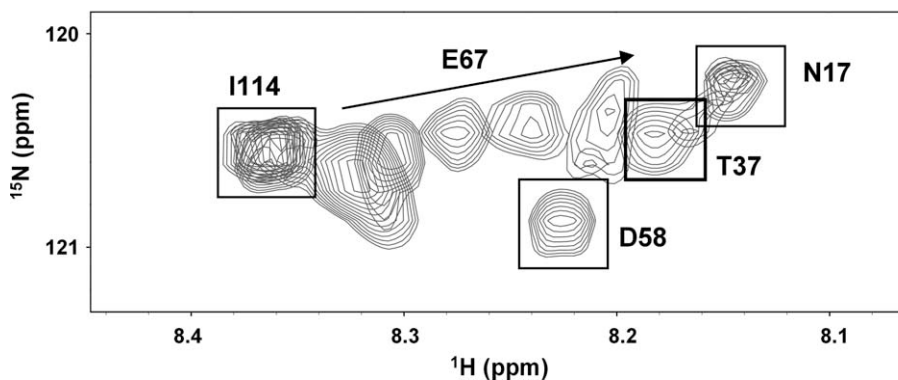


Fig. 5. Overlap of  $^{15}\text{N}$ - $^1\text{H}$  HSQC spectra of CaM-CD2-III-5G-52 at a selective region at different  $\text{La}^{3+}$  concentrations in 20 mM PIPES-20 mM KCl, pH 6.8. Upon the addition of  $\text{La}^{3+}$ , E67 moves upfield and the intensity of D58 decreases, while I114 (corresponding to I97 in CD2) and T37 have only minor changes.

type CD2 or the host protein parts in the engineered proteins (Figs. 3 and 5). Therefore,  $\text{La}^{3+}$  specifically interacts with residues from the inserted EF-loops.

In the  $\text{Tb}^{3+}$  FRET experiments, the addition of excess  $\text{La}^{3+}$  or  $\text{Ca}^{2+}$  reduces  $\text{Tb}^{3+}$  fluorescence dramatically, suggesting that both  $\text{La}^{3+}$  and  $\text{Ca}^{2+}$  are able to compete directly with  $\text{Tb}^{3+}$  for the same binding pocket [34,35]. Because of the negligible contributions from the host protein, through either conformational change or direct binding, and the much smaller conformational entropy penalty than that of the peptides, the observed metal affinities by grafting methods should more closely reflect the intrinsic ability of an isolated EF-loop without the interferences of the protein environment and cooperativity.

In summary, we have shown that the insertions of single EF-loops III and IV do not change the native structure of the host protein CD2.  $\text{La}^{3+}$  and  $\text{Ca}^{2+}$  compete with  $\text{Tb}^{3+}$  for the same binding pocket. In addition,  $\text{La}^{3+}$  and  $\text{Ca}^{2+}$  specifically interact with residues from the inserted EF-loop in CaM-CD2-III-5G-52. The  $\text{Ca}^{2+}$ -binding affinities of the EF-hand loops from the C-terminus of CaM have been obtained. EF-loop III has stronger metal binding affinities to  $\text{Ca}^{2+}$ ,  $\text{Tb}^{3+}$  and  $\text{La}^{3+}$  than EF-loop IV. In the future, detailed analysis will be carried out on our engineered EF-loops, including comparing them with CaM to estimate the contribution of cooperativity, analyzing the conformational differences of both EF-loops in the absence of metal ions, and investigating the effects of the protein environment on the  $\text{Ca}^{2+}$ -binding affinity of EF-hand motifs.

#### 4. Abbreviations

CD	circular dichroism
NMR	nuclear magnetic resonance
CD2	first domain of rat cluster of differentiation two
GST	glutathione-S-transferase

CaM	calmodulin
HSQC	heteronuclear single-quantum coherence
IPTG	isopropyl- $\beta$ -thiogalactoside
EGTA	ethylene glycol-bis( $\beta$ -aminoethylether)- $N,N,N',N'$ -tetraacetic acid

#### Acknowledgments

We thank Drs. Robert Kretsinger and James Prestegard for helpful discussion. We thank Sarah Shealy for the mass spectrometry. We appreciate the critical review from Dan Adams and the members in Dr. Jenny J. Yang's group. This work is supported in part by the NSF Grant MCB-0092486 and NIH GM 62999-1 to JJY.

#### Appendix A. Supplementary data

Supplementary data associated with this article can be found in the online version at [doi:10.1016/j.jinorgbio.2005.03.011](https://doi.org/10.1016/j.jinorgbio.2005.03.011).

#### References

- [1] J.K. Krueger, G.A. Olah, S.E. Rokop, G. Zhi, J.T. Stull, J. Trehwella, *Biochemistry* 36 (1997) 6017–6023.
- [2] M. Osawa, H. Tokumitsu, M.B. Swindells, H. Kurihara, M. Orita, T. Shibamura, T. Furuya, M. Ikura, *Nat. Struct. Biol.* 6 (1999) 819–824.
- [3] B.A. Seaton, J.F. Head, D.M. Engelman, F.M. Richards, *Biochemistry* 24 (1985) 6740–6743.
- [4] H. Sun, T.C. Squier, *J. Biol. Chem.* 275 (2000) 1731–1738.
- [5] Y. Xia, A.L. Tsai, V. Berka, J.L. Zweier, *J. Biol. Chem.* 273 (1998) 25804–25808.
- [6] M. Ikura, *Trends Biochem. Sci.* 21 (1996) 14–17.
- [7] H. Kawasaki, R.H. Kretsinger, *Protein Profile* 2 (1995) 297–490.

- [8] J.J. Falke, S.K. Drake, A.L. Hazard, O.B. Peersen, Q. Rev. Biophys. 27 (1994) 219–290.
- [9] M. Ikura, T. Hiraoki, K. Hikichi, T. Mikuni, M. Yazawa, K. Yagi, Biochemistry 22 (1983) 2573–2579.
- [10] S. Linse, S. Forsén, Adv. Sec. Mess. Phosph. Res. 30 (1995) 89–151.
- [11] M.R. Nelson, W.J. Chazin, Biometals 11 (1998) 297–318.
- [12] D.J. Wolff, P.G. Poirier, C.O. Brostrom, M.A. Brostrom, J. Biol. Chem. 252 (1977) 4108–4117.
- [13] J.R. Dedman, J.D. Potter, R.L. Jackson, J.D. Johnson, A.R. Means, J. Biol. Chem. 252 (1977) 8415–8422.
- [14] T.H. Crouch, C.B. Klee, Biochemistry 19 (1980) 3692–3698.
- [15] C.H. Keller, B.B. Olwin, D.C. LaPorte, D.R. Storm, Biochemistry 21 (1982) 156–162.
- [16] D. Burger, J.A. Cox, M. Comte, E.A. Stein, Biochemistry 23 (1984) 1966–1971.
- [17] W.D. Horrocks Jr., Method. Enzymol. 226 (1993) 495–538.
- [18] C.W. Hogue, J.P. MacManus, D. Banville, A.G. Szabo, J. Biol. Chem. 267 (1992) 13340–13347.
- [19] P.B. O'Hara, Photochem. Photobiol. 46 (1987) 1067–1070.
- [20] Y.S. Babu, J.S. Sack, T.J. Greenhough, C.E. Bugg, A.R. Means, W.J. Cook, Nature 315 (1985) 37–40.
- [21] R.W. Wallace, E.A. Tallant, M.E. Dockter, W.Y. Cheung, J. Biol. Chem. 257 (1982) 1845–1854.
- [22] M.C. Kilhoffer, D. Gerard, J.G. Demaille, FEBS Lett. 120 (1980) 99–103.
- [23] M.C. Kilhoffer, J.G. Demaille, D. Gerard, FEBS Lett. 116 (1980) 269–272.
- [24] C.L. Wang, P.C. Leavis, J. Gergely, Biochemistry 23 (1984) 6410–6415.
- [25] P. Mulqueen, J.M. Tingey, W.D. Horrocks Jr., Biochemistry 24 (1985) 6639–6645.
- [26] C.L. Wang, R.R. Aquaron, P.C. Leavis, J. Gergely, Eur. J. Biochem. 124 (1982) 7–12.
- [27] S. Linse, A. Helmersson, S. Forsén, J. Biol. Chem. 266 (1991) 8050–8054.
- [28] R.E. Klevit, D.C. Dalgarno, B.A. Levine, R.J. Williams, Eur. J. Biochem. 139 (1984) 109–114.
- [29] M.D. Tsai, T. Drakenberg, E. Thulin, S. Forsén, Biochemistry 26 (1987) 3635–3643.
- [30] H. Ouyang, H.J. Vogel, Biometals 11 (1998) 213–222.
- [31] J. Hu, X. Jia, Q. Li, X. Yang, K. Wang, Biochemistry 43 (2004) 2688–2698.
- [32] G. Borin, P. Ruzza, M. Rossi, A. Calderan, F. Marchiori, E. Peggion, Biopolymers 28 (1989) 353–369.
- [33] B.J. Marsden, G.S. Shaw, B.D. Sykes, Biochem. Cell Biol. 68 (1990) 587–601.
- [34] Y. Ye, H.W. Lee, W. Yang, S.J. Shealy, A.L. Wilkins, Z.R. Liu, I. Torshin, R. Harrison, R. Wohlhueter, J.J. Yang, Protein Eng. 14 (2001) 1001–1013.
- [35] Y. Ye, S. Shealy, H.W. Lee, I. Torshin, R. Harrison, J.J. Yang, Protein Eng. 16 (2003) 429–434.
- [36] H.W. Lee, W. Yang, Y. Ye, Z.R. Liu, J. Glushka, J.J. Yang, Biochim. Biophys. Acta 1598 (2002) 80–87.
- [37] P.C. Driscoll, J.G. Cyster, I.D. Campbell, A.F. Williams, Nature 353 (1991) 762–765.
- [38] W. Yang, L.M. Jones, L. Isley, Y. Ye, H.W. Lee, A. Wilkins, Z.R. Liu, H.W. Hellinga, R. Malchow, M. Ghazi, J.J. Yang, J. Am. Chem. Soc. 125 (2003) 6165–6171.
- [39] H.A. Chen, M. Pfuhl, B. Davis, P.C. Driscoll, J. Biomol. NMR 12 (1998) 457–458.
- [40] W. Yang, A.L. Wilkins, Y. Ye, Z.R. Liu, S.Y. Li, J.L. Urbauer, H.W. Hellinga, A. Kearney, P.A. van der Merwe, J.J. Yang, J. Am. Chem. Soc. 127 (2005) 2085–2093.
- [41] W. Yang, T. Tsai, M. Kats, J.J. Yang, J. Pept. Res. 55 (2000) 203–215.
- [42] B. Rajini, P. Shridas, C.S. Sundari, D. Muralidhar, S. Chandani, F. Thomas, Y. Sharma, J. Biol. Chem. 276 (2001) 38464–38471.
- [43] R.E. Reid, R.S. Hodges, J. Theor. Biol. 84 (1980) 401–444.
- [44] R.M. Procyshyn, R.E. Reid, J. Biol. Chem. 269 (1994) 1641–1647.
- [45] R.M. Procyshyn, R.E. Reid, Arch. Biochem. Biophys. 311 (1994) 425–429.
- [46] R.E. Reid, J. Biol. Chem. 265 (1990) 5971–5976.
- [47] X. Wu, R.E. Reid, Biochemistry 36 (1997) 8649–8656.
- [48] Y.S. Babu, C.E. Bugg, W.J. Cook, J. Mol. Biol. 204 (1988) 191–204.
- [49] P.J. Kraulis, J. Appl. Cryst. 24 (1991) 946–950.